

Classification of Physiography from ERTS Imagery*

Spatial information derived from ERTS-1 imagery of Kansas was highly correlated with physiography

INTRODUCTION

This investigation was conducted to determine if spatial frequency analysis of Earth Resources Technology Satellite (ERTS-1) imagery could provide an unbiased means of recognizing the character and nature of large-scale ground patterns in the image. Specifically considered was the determination of spatial frequency and orientational information from large-scale ground patterns in

The Osage Plains in the eastern part of the state are made up of a series of eastward-facing escarpments formed by outcrops of Pennsylvanian limestone and shales. The Flint Hills consist of a series of escarpments carved in outcrops of a series of chert-bearing Permian limestones that are very resistant to erosion. Dakota sandstone outcrops (Cretaceous) form the Smoky Hills upland in the North Central part of the state. Similarly, the

ABSTRACT: The potential application of optical data processing to ERTS imagery as a means for automatic identification of large-scale ground patterns was investigated. Spatial frequency distribution and orientational information were derived from ERTS-1 imagery of Kansas for each of 80 sample areas, each 37 km in diameter. The application of classification algorithms to this data reveals that a high degree of correlation exists between the physiography of a sample area and its frequency information. Specifically, the band of frequencies between 1.1 and 2.8 cycles/km appear to contain most of the information needed in distinguishing different physiographic regions.

Kansas by using ERTS-1 imagery as the input to an optical data processing system. Since the physiography and geology of Kansas are well known, use of this method would provide an objective means of identifying and classifying ground patterns and locating anomalous patterns.

CATEGORIES AND SAMPLE SITE LOCATION

Eight regions in Kansas (as adapted from Schoewe, 1949) are shown in Figure 1. Each physiographic unit is also an area of unique geologic character; each region is underlain by a dominant lithology which is reflected in a characteristic and unique topography.

* This work was supported by NASA Contract NAS 5-21822.

Blue Hills are formed by outcrops of Upper Cretaceous limestones and chinks.

Beyond the Blue Hills lie the High Plains, an accumulation of sediments derived through erosion from the Rocky Mountains to the west. Numerous aggrading streams swept eastward during the Tertiary, carrying and depositing sand and gravel and forming a vast outwash plain that is the present land surface. Even younger deposits occur in the various prairies and lowlands associated with the Arkansas River, some of which are covered with wind blown sand in the form of stabilized and active dunes. In the south-central part of the state are the Red Hills or Cimarron Breaks. These mark the border of the High Plains in the vicinity of the Cimarron River, which, with its tributaries, eroded into the red Per-

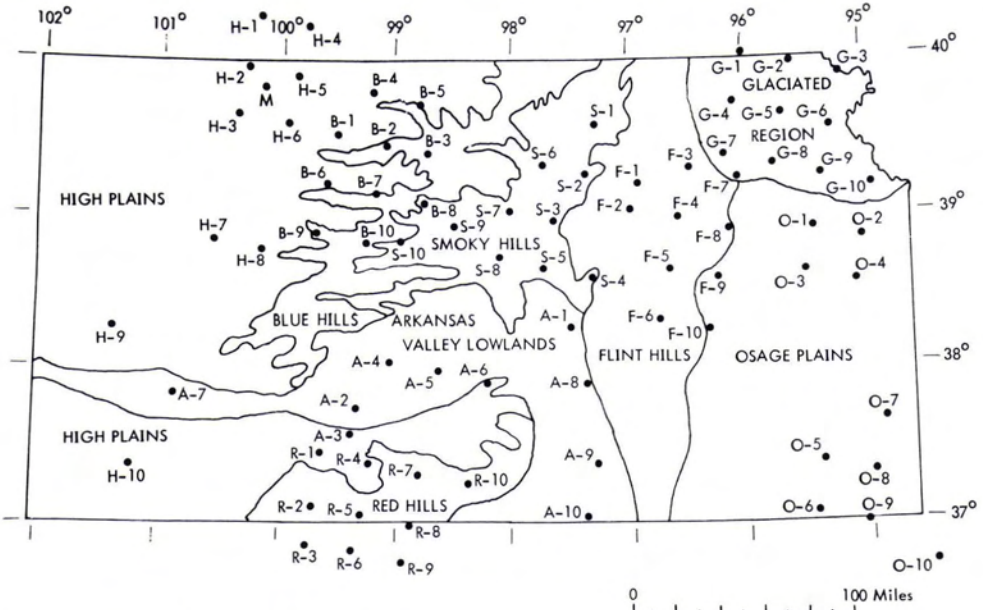


Fig. 1 Physiographic regions of Kansas (adapted from Schoewe, 1949) with sample site locations.

mian siltstones and shales that underlie the High Plains in that area. The extreme northeast corner of that state, occupied by the Kansan glacier during the Pleistocene, was resculptured to some extent and the area was covered to varying depths by glacial deposits. Thus the basically subtle surface structure of Kansas must be considered when using remote sensors to map the stratigraphic units or structure of the state.

Ten sample areas were chosen in each of these regions. The sample area center points are plotted in Figure 1. (Although some sample areas are in or overlap neighboring states, they remain in the same geologic category.) Each site has an alpha-numeric designation. F-1 refers to the first sample area in the Flint Hills; O-6 refers to the sixth sample area in the Osage Plains; etc. The sample area in the High Plains region of Kansas, designated "M" in Figure 1, was analyzed for all four MSS (Multi-Spectral Scanner) frequency bands (MSS 4,5,6,7) in order to determine the relative information content of each band. Band 5 images were found to contain the most information pertinent to this investigation (McCauley et al. 1975). Hence, for all other sample areas, MSS band 5 (0.6 - 0.7 microns) 70 mm positive transparencies were used in the analysis.

The 37-kilometer diameter of the sample area plus the size of the physiographic region determined the spacing of the sample areas within each category. The sample areas were

chosen from ERTS imagery recorded in the summer and fall of 1972. Detailed analysis of each sample area was performed and the results were presented in Ulaby (1973).

IMAGERY ANALYSIS

Basic physical optics and diffraction problems are discussed in Born and Wolf (1959), Goodman (1968), and Parrent and Thompson (1969). Optical systems similar to the one used in this investigation are discussed in Lee and Gossen (1971), and Read and Cannata (1974). Other investigations using optical diffraction analysis for image analysis are Stanley, Nienow and Lendaris (1969), and Lendaris and Stanley (1969), in which diffraction pattern sampling was used as a means to attain automatic target recognition; Davis and Preston (1972), McCullagh and Davis (1972), Pincus and Dobrin (1966), and Steckley (1972), in which optical diffraction analysis was used in geologic applications; and Read and Cannata (1974), in which one-dimensional data records were analyzed. Another investigation in which ERTS imagery is analyzed by diffraction pattern analysis is reported by Gramenopoulos (1973).

Each sample area on the ERTS image comprises ground patterns of characteristic spatial frequency and orientations (spatial frequencies here refer to variations of density on the image as a function of distance). Hence, if we decompose the image sample area into its component frequencies and plot

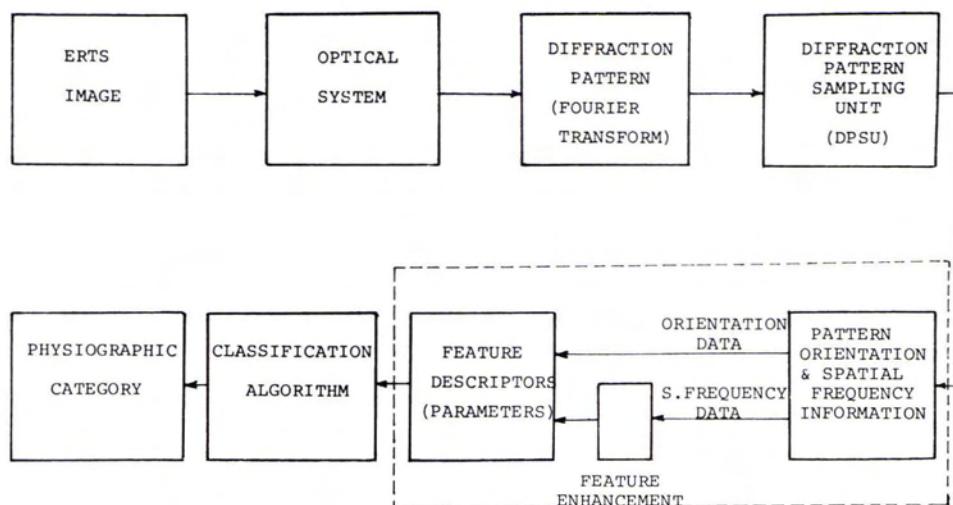


Fig. 2 Block diagram of optical processing and pattern recognition system.

their intensity distribution, and if we plot the "strength" of preferred orientations in the image versus angle, then we can describe the sample area by a set of numbers characteristic of the ground patterns.

A block diagram of the optical processing system, including the pattern recognition electronics, is shown in Figure 2. This figure diagrams the various steps necessary to derive sufficient quantitative information from the ERTS sample area to categorize that area.

The optical processor system (Figure 3) has three main elements: a laser, optics, and a Recognition Systems, Inc., Diffraction Pattern Sampling Unit (DPSU). An ERTS-1 70 mm positive transparency is used as the input to this system. A portion of the ERTS transparency (sample area) is illuminated by the incident laser beam, which is focused by the lens so that the point source produced by the spatial filter is imaged at a distance $z + f$ in

front of the lens. The light distribution in this plane is proportional to the Fourier transform of the transmittance function that describes the portion of the ERTS image illuminated by the beam. The intensity distribution (spatial spectrum) of the ERTS image is then sampled by the DPSU.

The DPSU consists of a 64-element photodiode array (Figure 4) used to detect the light intensity incident upon each element, and of electronics that amplify and digitize the output from each diode in the array. The diode array is composed of 32 wedge-shaped photodiodes and 32 annular ring photodiodes. The average intensity for each photodiode is recorded, calibrated, printed, and then plotted.

The spatial frequency in the transform plane is related to other system parameters by Ulaby (1973):

$$s = r/d\lambda$$

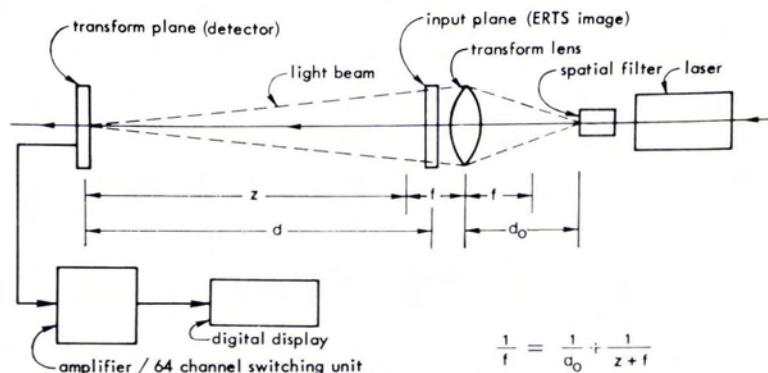


Fig. 3. System configuration.

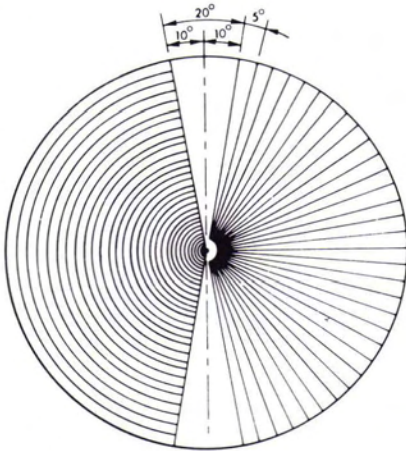


Fig. 4. Detector geometry.

where

- s = spatial frequency at a point r in the transform plane,
- r = distance in transform plane measured from optical axis,
- d = distance from image transparency to detector, and
- λ = wavelength of laser radiation = 6328\AA .

The spatial frequency from this calculation is converted to ground spatial frequency by using image-to-ground scale. The resulting curves plotted by the computer program are, then, intensity vs. frequency and intensity vs. angle. These are plotted in terms of ground spatial frequency in cycles per kilometer; direction is in compass degrees from north.

RESULTS OF EXPERIMENT

Spatial frequency curves obtained for each sample area were modified in order to enhance their ability to display salient features. An average spatial frequency curve was calculated for the 80 sample areas; the point-by-point ratio between this curve and each sample area frequency curve was determined, and these values were then plotted. Relative amplitudes of the various frequency components are greatly emphasized by using this method. The next section will demonstrate that these modified spatial frequency curves characterize the sample areas.

To this point, each sample has been described by a modified spatial frequency curve and an orientational curve. The progression from the ERTS sample areas to the modified spatial frequency and orientational curves is illustrated next.

Specific features in a sample area can be related to the spatial frequency and orienta-

tional information derived for it. Figure 5a shows a portion of ERTS-1 image no. 1076-16393-5. The circular section is sample area F-7 from the Flint Hills region of Kansas. Figure 5b illustrates the diffraction pattern associated with features in the sample area shown in Figure 5a as obtained with the optical processor. The primary feature of the diffraction pattern is a bright vertical distribution, A, that is due to the scan lines associated with the manner in which ERTS MSS images were obtained. Vertical distributions are not detected with the DPSU, however, since a 20 degree dead space exists in this region (see Figure 4). The intensity distribution in Figure 5b is sampled by using the DPSU described in the last section.

Normalized, calibrated spatial frequency (1) and orientational (2) curves are shown in Figure 5c. As noted, these plots are obtained by recording the light intensity at each photodiode in the detector array and then incorporating these data in a computer program. The spatial frequency curve, obtained from the ring-shaped photodiodes, gives the intensity of various spatial frequency components corresponding to features in the image sample area. The normalized intensity (shown here on a logarithmic scale) is recorded against ground spatial frequency in cycles/kilometer. The orientational curve, obtained from the wedge-shaped photodiodes, indicates the orientation of features in the sample area. The intensity, normalized with respect to the largest value, is recorded against the orientation clockwise in degrees from image north.

Figure 5d shows the modified spatial frequency curve obtained from the spatial frequency curve in Figure 5c, with amplitudes of the various frequency components greatly emphasized. The curve in Figure 5d shows that frequency component values around 0.4 and 1.0 cycles/km tend to predominate. In addition, peaks probably caused by characteristic features in the sample curve occur in the spatial frequency curve shown in Figure 5c of around 0.4 and 1.0 cycles/km, as verified by the sample area in Figure 5a. The light-toned band in this image represents the Kansas River flood plain, an area of intensive agriculture approximately 2.5 kilometers wide. Hence, its corresponding characteristic frequency is near $1/2.5 = 0.4$ cycles/km. The distribution around 1.0 is apparently produced by characteristic stream pattern frequencies. The orientational curve, (2) in Figure 5c, also has a number of characteristics related to features in the sample area.

One dominant peak at B, at approximately

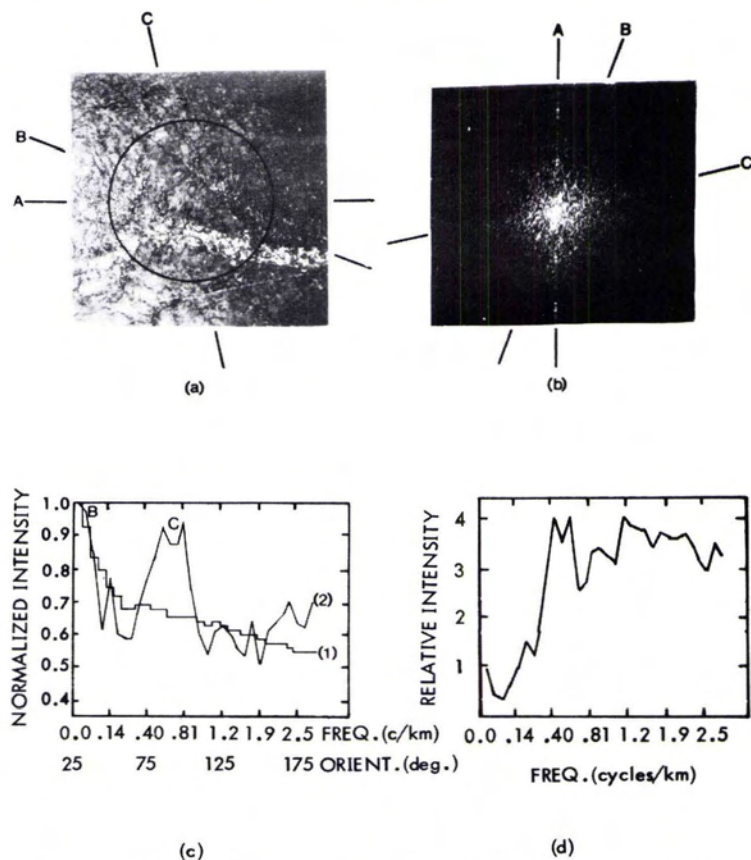


Fig. 5. Example showing progression of steps from portion of ERTS image No. 1076-16393-5 (a); to diffraction pattern (b); to digitized computer plots (c); to modified spatial frequency curve (d).

35 degrees, appears to result from the orientation of the Kansas River flood plain at approximately 30 to 35 degrees clockwise from west to the sample area. Thus, because of the nature of the system, this plain produces the distribution at B in Figure 5b which is oriented at 90 degrees away. The peak at C in curve 2 of Figure 5c, centered around 90 degrees, is due to the northward orientation of the field patterns and the general orientation of the major streams. Furthermore, the distribution at C in Figure 5c is also relatively wide, indicating the variation in stream orientations of around 90 degrees. Thus, features in the sample area can be related to characteristics in the diffraction pattern and in turn related to features in the spatial frequency and orientational curves.

CLASSIFICATION RESULTS

Various data processing schemes were developed to extract parameters from modified spatial and orientational curves and thus re-

duce the amount of information contained in them. These parameters describe the geologic or physiographic features that produce fluctuations in the curves. To determine how accurately these parameters characterize each sample area, they are used as input to pattern classification algorithms in order to categorize the sample areas.

The range of frequencies was divided into two bands: band 1 contains spatial frequencies between 0.0 and 0.9 cycles/km, and band 2 contains spatial frequencies between 1.1 and 2.8 cycles/km. This division essentially separates information due to high-frequency fluctuations caused by stream patterns in rough terrain, and from low-frequency information due to field patterns. Similarly, the range of orientational data was divided into four sectors, each corresponding to 40 degrees. Sector 1 provides data on pattern orientations that produce distributions between 25 and 65 degrees clockwise from north; sector 2, 65-105 degrees; sector 3,

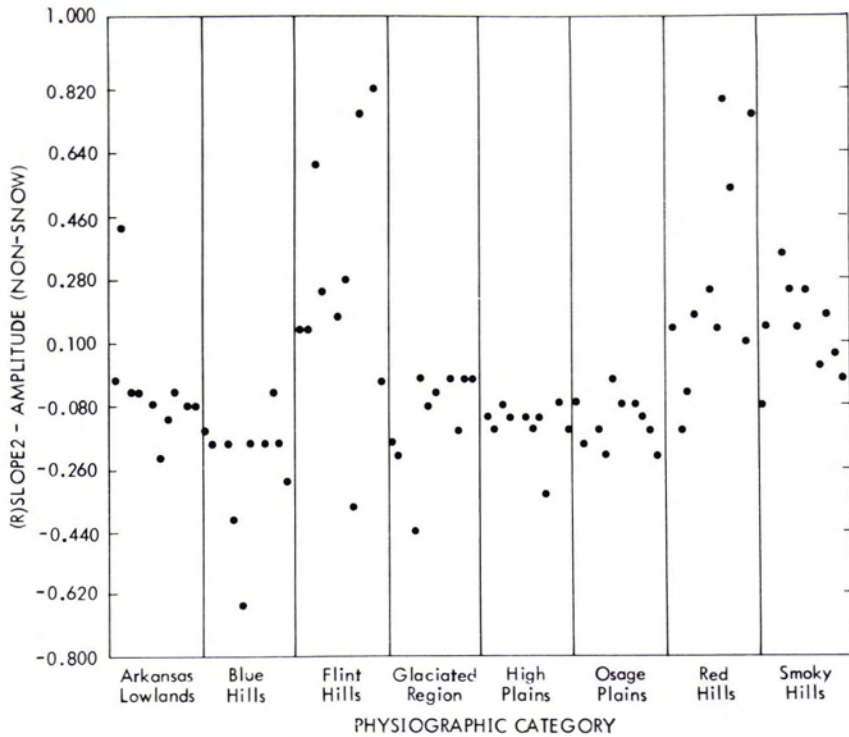


Fig. 6. Parameter plot using the parameter (R) SLOPE 2.

105-145 degrees; and sector 4, 145-185 degrees.

Parameters are extracted from the spatial frequency and orientational curves in each range. Each parameter for all 80 sample areas was plotted against its appropriate sample area category as obtained from Figure 1. One of these parameter plots is shown in Figure 6. Decision boundaries may be inserted into the parameter plots based on the distribution of the parameter's amplitudes. If a clear relationship exists between the amplitude of the parameter and the physiographic characteristics of the sample area, the decision boundary will discriminate between two large-scale physiographic ground patterns.

This was applied to the parameter labeled Slope 2, which is merely the slope of the regression line for the modified spatial frequency curve of the frequencies in band 2. As illustrated in Figure 6, a decision boundary that effectively separates the various categories may be inserted at approximately zero slope (+ 0.001). Sample areas from categories of relatively large high-frequency content (Flint Hills, Red Hills, Smoky Hills) yield a positive slope, whereas those from the other categories yield a negative value of this parameter. This identification experiment resulted in an accuracy of 92.5 percent with

only six incorrect identifications based on the original categorization of the sample areas.

Figure 7 illustrates how a further classification based upon the original physiographic regions can be made. Here a scattergram is made by plotting values of the parameter DARAN2 (area of the modified spatial frequency curve above the value 1.0 in band 2) versus values of SLOPE2. Values on this scattergram are keyed as follows:

- = Red Hills, Flint Hills and Smoky Hills,
- = Blue Hills
- = Glaciated region and Osage Plains, and
- = High Plains and Arkansas River Valley Lowland.

Each of these categories appears to be distributed in separate portions of the graph. We may insert decision boundaries into this group to separate the various categories, as was done previously in the one-dimensional case. When a region for each category is defined in terms of these boundaries, we may determine how accurately these two parameters classify each sample area; the results of this classification are shown in Table 1. In this case, the overall identification accuracy for each sample area is 80 percent.

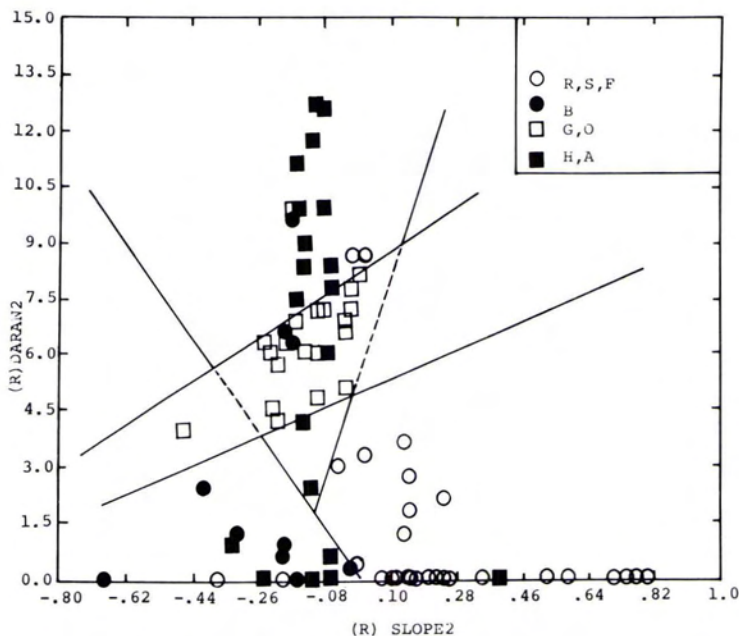


Fig. 7. Scattergram obtained using the parameters SLOPE2 and DARAN2.

Figure 8 shows the sample areas with respect to their identification based on Figure 7. Figure 8 (with sample area identification based on the key for Figure 7) shows that although the sample areas were identified with an accuracy of only 80 percent, in Kansas they appear to be clustered in terms of their identified categories. For instance, A-4, A-5, and A-6 are classified with the Blue Hills to the north, and H-8 is classified with the Blue Hills immediately to the east.

Various algorithms are available to automatically implement this classification. One scheme given in Fukunaga (1972) uses a regression-type algorithm to assign samples to various categories. Haralick and Shanmugan (1973) developed a program based on this algorithm that was used in an attempt to classify the sample areas; however, only limited success was achieved because of the relatively small number of samples used in this investigation.

CONCLUSIONS

Evidence presented in this study establishes that optical data processing of ERTS-1 images can be implemented to identify large-scale ground patterns in Kansas. Notably, the sample areas used in this investigation are not uniform, i.e., they do not display merely one dominant characteristic. Because each sample area is approximately 37

kilometers in diameter, the terrain may vary substantially within each sample area. Even given the "noise" associated with the sample areas, this method identifies the sample areas in terms of the original physiographic categories.

The manual interpretation of the spatial frequency and orientational curves shown here for one sample area (presented for all the sample areas in Ulaby, (1973)) demonstrates that this method of analysis can provide an unbiased means of evaluating the orienta-

TABLE 1. RESULT OF CLASSIFICATION OF SAMPLE AREAS BASED ON FIGURE 8.

Category	Hit	Missed	Total Samples	% Accuracy
R, S, F	25	5	30	83
B	7	3	10	70
G, O	19	1	20	95
H, A	13	7	20	65
Total	64	16	80	80

R—Red Hills
 S—Smoky Hills
 F—Flint Hills
 B—Blue Hills
 G—Glaciated Region
 O—Osage Plains
 H—High Plains
 A—Arkansas Lowlands

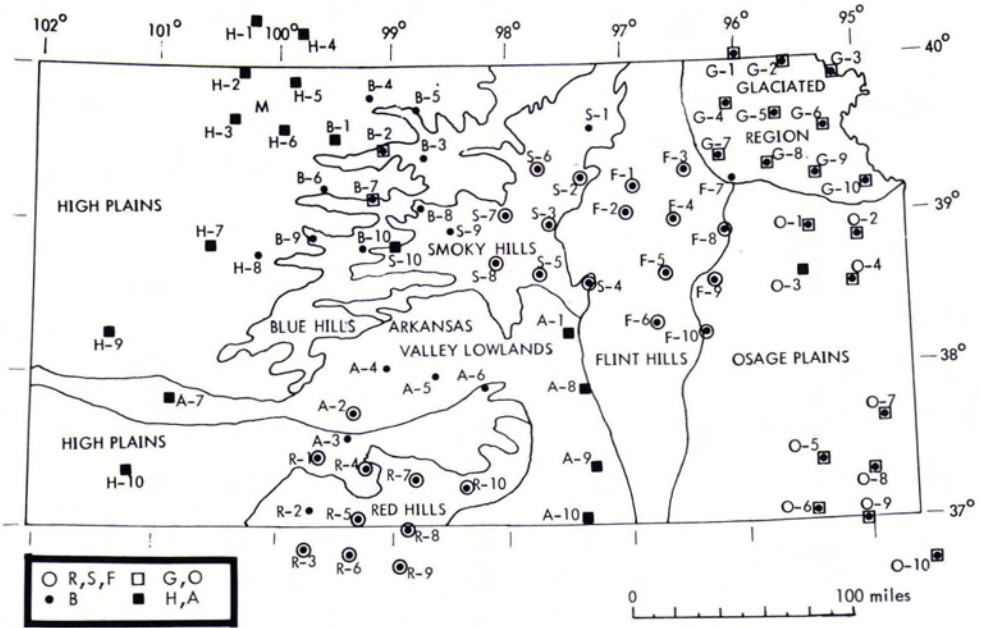


Fig. 8. Classification of sample areas based on Figure 7.

tions, natures of stream pattern, and other features apparent in the image.

The band of frequencies between 1.1 and 2.8 cycles/km appears to contain most of the information useful in distinguishing the various physiographic categories. For classifying the categories, the information contained in frequencies below 1.1 cycles/km is not apparent; conversely, the information in the frequencies from 3.1 to 5.8 cycles/km appears to discriminate between categories almost as well as the band from 1.1 to 2.8 cycles/km but only for certain parameters. Sample pattern orientational information is not so useful in discrimination between categories as the spatial frequency information.

It should be noted here that the method of analysis used in this investigation is deliberately general. These methods and algorithms could be applied to various other image analysis or categorization problems, because the method of analysis shown here is image independent and can be completely automated.

REFERENCES

- Born, M. and E. Wolf, (1959), *Principles of Optics*, Pergamon Press, New York.
- Davis, J. C. and F. W. Preston, (1972), "Optical Processing: An Alternative to Digital Computing," The Geological Society of America, Inc., Special Paper 146.
- Fukunaga, K., (1972), *Introduction to Statistical Pattern Recognition*, Academic Press, New York.
- Goodman, J. W., (1968), *Introduction to Fourier Optics*, McGraw-Hill Book Co., New York.
- Gramenopoulos, Nicholas, (1973), "Terrain Type Recognition Using ERTS-1 MSS Images," ERTS-1 Symposium, March 5-9, 1973, New Carrollton, Maryland.
- Haralick, R. M. and K. Shanmugan, (1973), "Computer Classification of Reservoir Sandstones," *IEEE Trans. on Geoscience Electronics*, vol. GE-11, no. 4, October.
- Lee, T. C. and D. Gossen, (1971), "Generalized Fourier-Transform Holography and Its Applications," *Applied Optics*, vol. 10, no. 4, April.
- Lendaris, G. G. and G. D. Stanley, (1969), "Diffraction-Pattern Sampling for Automatic Pattern Recognition," *Seminar Proceedings, Pattern Recognition Studies*, Society of Photo-Optical Instrumentation Engineers, June 9-10, New York.
- McCauley, J., D. Egbert, J. McNaughton and F. T. Ulaby, (1975), "Stream Pattern Analysis Using Optical Processing of ERTS Imagery of Kansas," *Modern Geology*, (in press).
- McCullah, M. J. and J. C. Davis, (1972), "Optical Analysis of Two-Dimensional Patterns," *Annals of the Association of American Geographers*, vol. 62, no. 4, December.
- Parrent, G. B., Jr. and B. J. Thompson, (1969), *Physical Optics Notebook*, Society of Photo-Optical Instrumentation Engineers.
- Pincus, H. J. and M. B. Dobrin, (1966), "Geological Applications of Optical Data Processing," *Journal of Geophysical Research*, vol. 71, p. 4861-4869.
- Preston, Kendall, (1972), *Coherent Optical Computers*, McGraw-Hill Book Co., New York.

- Read, A. A. and R. F. Cannata, (1974), "Coherent Analysis Enriches Yield from 1-D Data Records," *Laser Focus*, p. 65, March.
- Schoewe, W. H., (1949), "The Geography of Kansas, Pt. 2, Physical Geography," *Kansas Academy of Science Transactions*, vol. 52, no. 3, pp. 261-333.
- Shulman, A. R., (1970), *Optical Data Processing*, John Wiley & Sons, Inc., New York.
- Stanley, G. L., W. C. Nienow, and G. G. Lendaris, (1969), "SARF, An Interactive Signature Analysis Research Facility," AC-DRL Techni-

cal Report TR 69-15, Santa Barbara, California, March.

- Steckley, R. C., (1972), "Determination of Paleotonic Principle Stress Direction, Including Analysis of Joints by Optical Diffraction," U. S. Dept. of Interior, Bureau of Mines, PGH, PA. 18036, U. S. Govt. Printing Office: 1972-709-309:551.
- Ulaby, F. T., (1973), "Ground Pattern Analysis in the Great Plains," CRES Technical Report 2266-4, University of Kansas Center for Research, Inc., Lawrence, July.

Engineering Reports

Business—Equipment—Literature

Gordon R. Heath

WILD INTRODUCES EK22 DATA ACQUISITION SYSTEM

Wild Heerbrugg has designed the EK22 data acquisition system for the plotting instruments Wild A7, A8, A10, A40, and B8/B8S. Thanks to its great flexibility, the EK22 can be connected to all types of data-output and data-processing devices.



Its main features are easy operation, a system that can be further developed, low trouble incidence, and ease of servicing. Its most important applications are in aerial triangulation and control-point densification, large-scale cadastral surveys, digital terrain models, registrations of profiles and cross-sections in road and railway construction, measurement of volumes, and coordinate measurement in industrial applications of photogrammetry. For more information contact Wild Heerbrugg Ltd., CH-9435 Heerbrugg, Switzerland.

ALTEK ANNOUNCES AC 74 PHOTOGRAMMETRIC DATA ACQUISITION SYSTEM

ALTEK announces a digitizer designed specifically for interface to stereoplotters, comparators, and coordinatographs. The standard model avoids a great amount of complex circuitry, featuring instead low cost and simplicity of operation. Using rotary or linear encoder input, the AC 74 will display up to four 6-digit values and transmit the in-

formation to any digital recording device (card punch, magnetic tape recorder, etc.) or computer. Complete system prices including interfaces begin at \$6,750.00 (lower for the 2-axis model AC 72). ALTEK Corp. is located at 2141 Industrial Parkway, Silver Spring, MD, 20904.

FAIRCHILD TO PRODUCE FILM TITLERS FOR AIR FORCE

A contract for \$700,000 to supply nine automatic film titling systems to the United States Air Force has been awarded by the Directorate of Procurement & Production at Hill AFB, Utah, to the Space & Defense Systems Division of Fairchild Camera



& Instrument Corporation. The contract covers the first production run of nine systems of an automatic film titling system developed by Fairchild for the Air Force in 1973. The Series F-699B titlers will be